

TWO-DIMENSIONAL MODEL OF TRANSFER PROCESSES ON A BUBBLE PLATE IN MULTICOMPONENT RECTIFICATION

A. G. Laptev^a and V. A. Danilov^b

UDC 66.048.3

A mathematical model of the process of rectification of a multicomponent mixture on a bubble plate is presented. The transfer processes in the two-phase gas–liquid flow are described using a two-liquid model with account for the distinctive features of the phase interaction on the plate. The results of calculations according to the Young model are compared to the experimental data on the rectification of an N-hexane–ethanol–methylcyclopentane–benzene mixture on a sieve plate 0.302 m in diameter.

The technology of production of various chemical products involves rectification of multicomponent mixtures in plate-type column apparatuses. Determination of the separative power of the column is associated with mathematical description of the transfer processes in a two-phase flow on the plates. There are idealized and semiempirical models of the transfer processes on the plates, such as ideal displacement in the gas phase and complete mixing in the liquid phase [1, 2], and diffusion [3] and cellular [4] models in the gas and liquid phases.

The drawback of the semiempirical models lies in the need to experimentally determine their parameters. The application of multiphase models, providing a basis for modern CFD commercial packages, is limited by the complexity of closure and solution of a complete system of transfer equations in phases.

Many publications [5–7] have been devoted to numerical investigation of the hydrodynamics of a gas–liquid flow based on the two-liquid model in bubble columns. Solution of three-dimensional equations of motion of the gas–liquid flow on a sieve plate has been obtained in [8] with the use of the CFX-4 commercial package. The two-dimensional model of the hydrodynamics of a two-phase flow on the plate where the motion of only the continuous (liquid) phase is considered has been suggested.

One basic problem in describing the transfer processes in the present system is the complex character of motion of the dispersed phase (motion of jets, dispersion, coalescence, and grinding), which hinders solution of the complete system of transfer equations in the two-phase flow. Therefore, the construction of a mathematical model of the process of separation on a contact device with a minimum use of experimental data is a pressing problem.

In the present work, we suggest a model of transfer processes that is constructed on the basis of the two-liquid model [5–10] with account for the distinctive features of the phase interaction on the plate.

According to the two-liquid model, for the k -phase we have:
the equation of motion [10]

$$\frac{\partial (\alpha_k \rho_k \mathbf{V}_k)}{\partial t} + \nabla \cdot (\alpha_k \rho_k \mathbf{V}_k \mathbf{V}_k) = -\alpha_k \nabla P_k + \nabla \cdot \alpha_k (\boldsymbol{\tau}_k) + \alpha_k \rho_k g + \mathbf{V}_{ks} \Gamma_k - \nabla \alpha_k \cdot \boldsymbol{\tau}_s + \mathbf{r}_{pk}; \quad (1)$$

the continuity equation [10]

$$\frac{\partial (\alpha_k \rho_k)}{\partial t} + \nabla \cdot (\alpha_k \rho_k \mathbf{V}_k) = \Gamma_k; \quad (2)$$

the law of conservation of the component mass [7]

^aKazan State Power-Engineering University, Kazan, Russia; ^bKazan State Technological University, Kazan, Russia; email: dvaleri@yandex.ru. Translated from *Inzhenerno-Fizicheskii Zhurnal*, Vol. 76, No. 4, pp. 66–72, July–August, 2003. Original article submitted October 11, 2001; revision submitted February 22, 2002.

$$\frac{\partial (\rho_k \alpha_k C_k)}{\partial t} + \nabla \cdot (\rho_k \alpha_k \mathbf{V}_k C_k) = \nabla \cdot (\rho_k \alpha_k ([D_k] + [D_{tk}]) \text{grad } C_k) + r_{ck}; \quad (3)$$

the equation of heat transfer [10]

$$\frac{\partial (\alpha_k \rho_k H_k)}{\partial t} + \nabla \cdot (\alpha_k \rho_k H_k \mathbf{V}_k) = \nabla \cdot \alpha_k (q_k + q_{tk}) + \alpha_k \frac{DP_k}{Dt} + H_{ks} \Gamma_k + \Phi_k + r_{hk}. \quad (4)$$

Since the change in the thermophysical properties of the phases on the plate is insignificant, the equation of enthalpy transfer can be written with the use of temperature. The terms $\frac{DP_k}{Dt}$ and Φ_k in Eq. (4), because of their insignificance, can be neglected.

The tensor of tangential stresses in the liquid phase τ_{liq} [5] has the form

$$\tau_{\text{liq}} = -\mu_{\text{eff,liq}} \left[\nabla \mathbf{V}_{\text{liq}} + (\nabla \mathbf{V}_{\text{liq}})^t - \frac{2}{3} [I] (\nabla \cdot \mathbf{V}_{\text{liq}}) \right]. \quad (5)$$

The effective viscosity of the liquid phase $\mu_{\text{eff,liq}}$ is equal to

$$\mu_{\text{eff,liq}} = \mu_{\text{liq}} + \mu_{\text{t,liq}} + \mu_{\text{b,liq}}. \quad (6)$$

To calculate the component of the coefficient of turbulent viscosity, which takes into account the layer turbulence in motion of bubbles, we suggest the following equation [5]:

$$\mu_{\text{b,liq}} = C_b \rho_{\text{liq}} \phi d_b |\mathbf{V}_g - \mathbf{V}_{\text{liq}}|. \quad (7)$$

Generally, the interphase-interaction force $\mathbf{r}_{\text{p,liq}}$ includes several forces: the resistance force, the buoyancy force, the virtual-mass force, and others. A comparison of the experimental results to the numerical calculations of $\mathbf{r}_{\text{p,liq}}$, carried out in [5] according to different procedures, has shown that in the bubbling zone, the force $\mathbf{r}_{\text{p,liq}}$ determined by the resistance force [5] is predominant:

$$\mathbf{r}_{\text{p,liq}} = -\frac{3}{4} \phi (1 - \phi) \rho_{\text{liq}} \frac{C_d}{d_b} |\mathbf{V}_g - \mathbf{V}_{\text{liq}}| (\mathbf{V}_g - \mathbf{V}_{\text{liq}}). \quad (8)$$

It is known [11] that when the column diameter is more than 1.5 m, the nonuniformity of the phase distribution becomes significant. For the plate with a diameter less than 1.5 m, under the assumption of a uniform distribution of the dispersed phase in the two-phase flow, we have $\phi = \text{const}$. A foamy regime of operation of a crossflow-type plate with overflows is characterized by a fully developed turbulence in the liquid phase. Taking the mixing over the height in the liquid phase to be complete for this regime, we write

$$\frac{\partial u_{\text{liq}}}{\partial z} = 0, \quad \frac{\partial v_{\text{liq}}}{\partial z} = 0, \quad \frac{\partial w_{\text{liq}}}{\partial z} = 0, \quad \frac{\partial C_{\text{liq}}}{\partial z} = 0, \quad \frac{\partial T_{\text{liq}}}{\partial z} = 0. \quad (9)$$

Under steady-state operating conditions of the column, the transfer processes in the two-phase flow on the contact device are stationary. With allowance for the assumptions made, the equations of transfer of momentum (1) and (2), mass (3), and heat (4) for the liquid phase are transformed to the form

$$\begin{aligned} u_{\text{liq}} \frac{\partial u_{\text{liq}}}{\partial x} + v_{\text{liq}} \frac{\partial u_{\text{liq}}}{\partial y} &= \frac{1}{\rho_{\text{liq}}} \frac{\partial P}{\partial x} + \frac{\partial}{\partial x} \left[\frac{\mu_{\text{eff,liq}}}{\rho_{\text{liq}}} \frac{\partial u_{\text{liq}}}{\partial x} \right] + \frac{\partial}{\partial y} \left[\frac{\mu_{\text{eff,liq}}}{\rho_{\text{liq}}} \frac{\partial u_{\text{liq}}}{\partial y} \right] + \frac{r_{\text{p,liq}x}}{\rho_{\text{liq}} (1 - \phi)}, \\ u_{\text{liq}} \frac{\partial v_{\text{liq}}}{\partial x} + v_{\text{liq}} \frac{\partial v_{\text{liq}}}{\partial y} &= \frac{1}{\rho_{\text{liq}}} \frac{\partial P}{\partial y} + \frac{\partial}{\partial x} \left[\frac{\mu_{\text{eff,liq}}}{\rho_{\text{liq}}} \frac{\partial v_{\text{liq}}}{\partial x} \right] + \frac{\partial}{\partial y} \left[\frac{\mu_{\text{eff,liq}}}{\rho_{\text{liq}}} \frac{\partial v_{\text{liq}}}{\partial y} \right] + \frac{r_{\text{p,liq}y}}{\rho_{\text{liq}} (1 - \phi)}; \end{aligned} \quad (10)$$

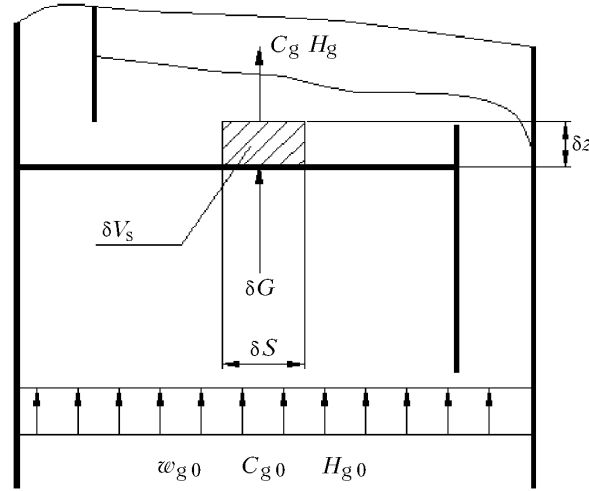


Fig. 1. Scheme of motion of the vapor flow in the separated volume of the two-phase flow on the crossflow-type plate.

$$\frac{\partial u_{\text{liq}}}{\partial x} + \frac{\partial v_{\text{liq}}}{\partial y} = \frac{\Gamma_{\text{liq}}}{\rho_{\text{liq}} (1 - \varphi)}; \quad (11)$$

$$u_{\text{liq}} \frac{\partial C_{\text{liq}}}{\partial x} + v_{\text{liq}} \frac{\partial C_{\text{liq}}}{\partial y} = \frac{\partial}{\partial x} \left[([D_{\text{liq}}] + D_{\text{t,liq}} [I]) \frac{\partial C_{\text{liq}}}{\partial x} \right] + \frac{\partial}{\partial y} \left[([D_{\text{liq}}] + D_{\text{t,liq}} [I]) \frac{\partial C_{\text{liq}}}{\partial y} \right] + \frac{r_{\text{c,liq}}}{\rho_{\text{liq}} (1 - \varphi)}; \quad (12)$$

$$u_{\text{liq}} \frac{\partial T_{\text{liq}}}{\partial x} + v_{\text{liq}} \frac{\partial T_{\text{liq}}}{\partial y} = \frac{\partial}{\partial x} \left[(a_{\text{liq}} + a_{\text{t,liq}}) \frac{\partial T_{\text{liq}}}{\partial x} \right] + \frac{\partial}{\partial y} \left[(a_{\text{liq}} + a_{\text{t,liq}}) \frac{\partial T_{\text{liq}}}{\partial y} \right] + \frac{r_{\text{h,liq}}}{c_{p\text{liq}} \rho_{\text{liq}} (1 - \varphi)}. \quad (13)$$

A distinctive feature of the motion of the two-phase gas-liquid flow on the bubble plate is that the velocity of the dispersed phase is much higher than the velocity of the continuous phase, $|\mathbf{V}_g| \gg |\mathbf{V}_{\text{liq}}|$. The gas in the liquid layer on the plate moves mainly in the vertical direction. With account for the cross motion of the phases, we have $w_g \gg u_g$ and $w_g \gg v_g$ for the components of the vector velocity \mathbf{V}_g in the vapor phase. Then, from Eq. (8) it follows that the components of the interphase-interaction force $\mathbf{r}_{\text{p,liq}}$ in projection onto the plate plane, because of their smallness, can be taken to be equal to zero:

$$r_{\text{p,liq}x} \approx 0, \quad r_{\text{p,liq}y} \approx 0. \quad (14)$$

Evaluation of the terms in the equation of mass transfer (3) for the vapor phase ($k \equiv g$) shows that

$$w_g \frac{\partial C_g}{\partial z} \gg u_g \frac{\partial C_g}{\partial x}, \quad w_g \frac{\partial C_g}{\partial z} \gg v_g \frac{\partial C_g}{\partial y}, \quad w_g \frac{\partial C_g}{\partial z} \gg ([D_g] + D_{\text{t,g}} [I]) \frac{\partial^2 C_g}{\partial z^2}. \quad (15)$$

After the evaluation is performed, Eq. (3) for the vapor phase takes the form

$$w_g \frac{\partial C_g}{\partial z} = \frac{r_{\text{c,g}}}{\rho_g \varphi}. \quad (16)$$

Let us consider a two-phase mixture of volume δV_s on a bubble plate (Fig. 1). We replace the derivative in Eq. (16) by the finite difference $\partial C_g / \partial z \approx (C_g - C_{g0}) / \delta z$ and multiply both sides by $\delta S \rho_g$. Then we have

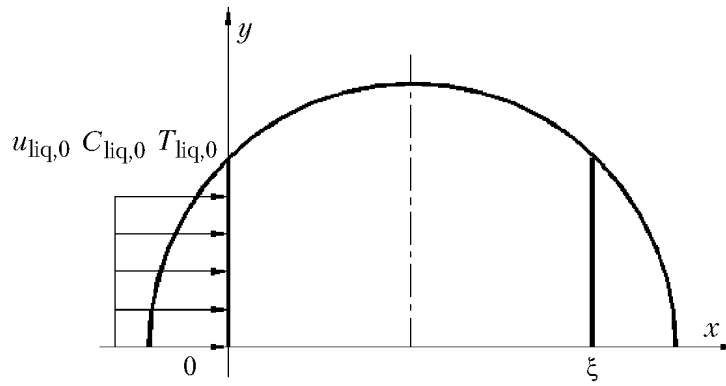


Fig. 2. Two-dimensional model of the plate.

$$(\delta S \rho_g) w_g \frac{C_g - C_{g0}}{\delta z} = \frac{r_{c,g}}{\rho_g \phi} (\delta S \rho_g) \quad (17)$$

or

$$\delta G (C_g - C_{g0}) = \delta M_g. \quad (18)$$

Similarly, we obtain the equation of conservation of heat in the vapor phase for the volume δV_s in the form

$$\delta G (H_g - H_{g0}) = \delta Q_g. \quad (19)$$

The mass source of the i th component $r_{c,liq,i}$ in the liquid phase is

$$r_{c,liq,i} = \frac{\delta M_{liq,i}}{\delta V_s}, \quad \delta M_{liq,i} = \delta V_{liq} \rho_{liq} \sum_{j=1}^{m-1} K_{liq,j} (C_{liq,j}^* - C_{liq,j}). \quad (20)$$

The column vector of the mass source $r_{c,g}$ in the vapor phase is

$$r_{c,g} = -r_{c,liq}. \quad (21)$$

The heat source $r_{h,liq}$ in the liquid phase is

$$r_{h,liq} = \frac{\delta Q_{liq}}{\delta V_s}, \quad \delta Q_{liq} = K_h (T_g - T_{liq}) \delta V_s. \quad (22)$$

The heat source $r_{h,g}$ in the vapor phase is

$$r_{h,g} = -r_{h,liq}. \quad (23)$$

For the system of equations (10)–(13) we establish the following boundary conditions (Fig. 2):

$x = 0$, $u_{liq} = u_{liq0}$, $v_{liq} = 0$, $P = P_0$, $C_{liq} = C_{liq0}$, and $T_{liq} = T_{liq0}$ (entrance to the plate);

$x = \xi$, $\partial u_{liq}/\partial x = 0$, $\partial v_{liq}/\partial x = 0$, $\partial C_{liq}/\partial x = 0$, and $\partial T_{liq}/\partial x = 0$ (exit from the plate);

$y = 0$, $\partial u_{liq}/\partial y = 0$, $v_{liq} = 0$, $\partial C_{liq}/\partial y = 0$, and $\partial T_{liq}/\partial y = 0$ (symmetry axis);

$y_w = f(x)$, $u_{tliq} = 0$, $v_{liq} = 0$, $\partial C_{liq}/\partial n = 0$, and $\partial T_{liq}/\partial n = 0$ (on the column wall).

To close the system of equations (10)–(13), it is necessary to determine the characteristics of turbulent exchange $\mu_{t,liq}$, $D_{t,liq}$, and $a_{t,liq}$ and the volumetric coefficients of mass and heat transfer.

Based on the theory of isotropic turbulence [12], we obtain an expression for calculating the coefficient of turbulent viscosity:

$$v_{t,liq} = 1.1 \frac{u_{f,liq}^4}{\varepsilon}. \quad (24)$$

In the core of the liquid phase, using the approximate equality $Pr_t \approx Sc_t \approx 1$, we have $v_{t,liq} \approx D_{t,liq} \approx a_{t,liq}$.

For determination of the matrix of mass-transfer coefficients $[\beta]$ we employ the Toor–Stewart–Prober method [13, 14], according to which one can use mass-transfer models obtained for binary mixtures for calculation of the diagonal matrix elements of the equimolar mass-transfer coefficients $[\check{\beta}]$. In [12], the following equation is recommended for calculating these elements:

$$\check{\beta}_i = \frac{u_f [S_b (\rho_g W_b^2/2 + \rho_{liq} g h_s) - \rho_g S W^2/2]}{\arctan \sqrt{R_1} Sc_i \sqrt{R_1} (u_f^2 \rho + 2\sigma/R_e) S_a h_s}. \quad (25)$$

The transition from the diagonal matrix $[\check{\beta}]$ to the square matrix of mass-transfer coefficients $[\beta]$ is performed according to the Sylvester theorem [15]. The influence of the transverse mass flux on the mass-transfer coefficients in the non-equimolar process is taken into account with the use of the correcting matrix Ξ [16]:

$$[\beta^\bullet] = [\beta] [\Xi]. \quad (26)$$

To calculate the volumetric heat-transfer coefficients in the bubble layer, the following equation was obtained in [12]:

$$\alpha = \frac{u_f [S_b (\rho_g W_b^2/2 + \rho_{liq} g h_s) - \rho_g S W^2/2]}{\arctan \sqrt{R_1} Pr \sqrt{R_1} (u_f^2 \rho + 2\sigma/R_e) S_a h_s} \rho C_p. \quad (27)$$

With allowance for the transverse mass flux [16], the heat-transfer coefficients are calculated from the formula

$$\alpha^\bullet = \alpha \Xi_h. \quad (28)$$

The volumetric heat-transfer coefficients K_h^\bullet and their matrix $[K_{liq}^\bullet]$ are determined from the equation of phase-resistance additivity [16].

The equilibrium in the vapor–liquid system was calculated using the IVC-SEP package [17]. The minimum of experimental data needed for calculations includes the data of hydraulic tests of the plate (height of a static liquid column, resistance of dry and wetted plates).

The equations of motion (10) and (11) for the continuous phase of the two-phase flow on the plate were calculated using the commercial CFD package Flow3D [18]. We simulated the motion of the single-phase flow with a prescribed effective viscosity and with the boundary conditions on the plate. The mass flux of the component N_i , required for determination of the total mass source Γ_{liq} and the correcting factors Ξ and Ξ_h , can be calculated according to the well-known procedure [16]. In the calculations, we neglect the total mass source Γ_{liq} because of its smallness.

The liquid-phase velocity profile obtained by solution of the equation of motion on the plate was applied to calculation of the fields of concentrations and temperatures following our own program composed in Fortran with the use of IMSL subprograms [19]. The concentrations of the components were found here through the numerical solution of the equation of multicomponent mass transfer (10) in combination with the equation of material balance (19) in the gas phase for the crossflow-type plate. The temperature field in the liquid phase on the plate was determined by solution of the heat-transfer equation (13) together with the heat-balance equation (19) in the gas phase for the crossflow-type plate.

The model suggested was used for calculation of the multicomponent rectification on the bubble plate according to the data of [20]. The experimental data on the rectification of the *n*-hexane-ethanol–methylcyclopentane–benzene

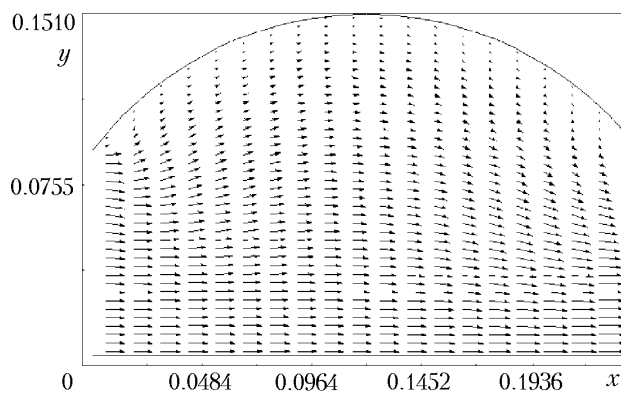


Fig. 3. Liquid-velocity profile on the plate (liquid flow rate 913.74 kg/h, steam consumption 277.99 kg/h, column diameter 0.302 m, $h_s = 0.016$ m, and $v_{t,liq} = 0.00452$ m²/sec).

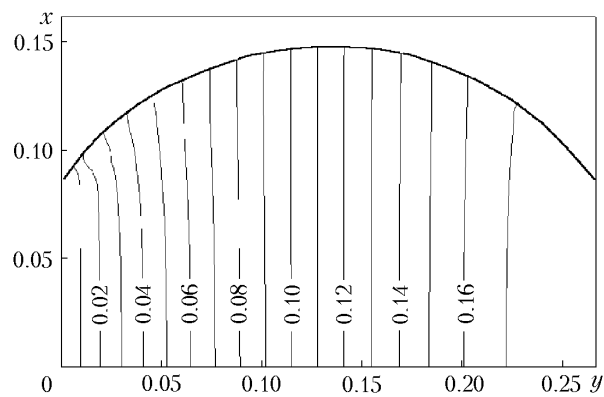


Fig. 4. Profile of the concentration of *n*-hexane $(C_{liq} - C_{liq0}) / (C_{liq}^* - C_{liq0})$ in the liquid phase on the plate (liquid flow rate 913.74 kg/h, steam consumption 277.99 kg/h, column diameter 0.302 m, $h_s = 0.016$ m, $C_{liq0} = 0.47$ mol.fractions, $C_{liq}^* = 0.4984$ mol.fractions, and $D_{t,liq} = 0.00452$ m²/sec).

TABLE 1. Comparison of the Experimental Concentrations of the Components on the Plate [20] and of Those Calculated by the Model (in mole fractions) in Multicomponent Rectification

Sampling point	Component	Experiment [20]			Calculation by the model		
		I	II	III	I	II	III
Angle 0°	<i>n</i> -Hexane	0.468	0.44	0.429	0.4707	0.44	0.4173
Radius 95 mm	Ethanol	0.154	0.24	0.278	0.1524	0.24	0.3066
$x = 26$ mm	MCP	0.161	0.138	0.131	0.1544	0.138	0.1402
$y = 0$ mm	Benzene	0.217	0.182	0.162	0.2225	0.182	0.1359
Angle 90°	<i>n</i> -Hexane	0.476	0.44	0.429	0.4731	0.44	0.4211
Radius 95 mm	Ethanol	0.144	0.24	0.278	0.1457	0.24	0.2931
$x = 121$ mm	MCP	0.159	0.138	0.131	0.1614	0.138	0.1398
$y = 95$ mm	Benzene	0.221	0.182	0.162	0.2198	0.182	0.1460
Angle 180°	<i>n</i> -Hexane	0.472	0.44	0.429	0.4745	0.44	0.4240
Radius 95 mm	Ethanol	0.145	0.24	0.278	0.1428	0.24	0.2814
$x = 216$ mm	MCP	0.162	0.138	0.131	0.1613	0.138	0.1394
$y = 0$ mm	Benzene	0.221	0.182	0.162	0.2214	0.182	0.1552
Angle 270°	<i>n</i> -Hexane	0.475	0.44	0.429	0.4731	0.44	0.4211
Radius 95 mm	Ethanol	0.146	0.24	0.278	0.1457	0.24	0.2931
$x = 121$ mm	MCP	0.158	0.138	0.131	0.1614	0.138	0.1398
$y = -95$ mm	Benzene	0.221	0.182	0.162	0.2198	0.182	0.1460

Note: MCP, methylcyclopentane; I, liquid; II, vapor at the entrance; III, vapor at the exit.

mixture were obtained in [20] for a 0.302-m-diameter column with three sieve plates. Work [20] also contains the design parameters of the plate, the values of the height of the static liquid column, and the flow rate and composition of the phases on the plate. Figure 3 illustrates the liquid-phase-velocity field calculated by the model with the use of the commercial CFD Flow3D package. A 20×40 -partition grid is employed. The liquid velocity at the entrance to the plate is 0.15 m/sec. As can be seen from Fig. 3, the complex character of liquid motion on the plate (expansion and contraction of the flow) leads to the formation of stagnant zones near the column walls. Using the commercial CFD Flow3D package, we also simulated numerically the pulse injection of a tracer into the liquid flow at the entrance to the plate. The initial condition for the nonstationary equation of tracer transfer was assigned in the form of

the Dirac δ function. The processing of the response curve according to the well-known procedures [2, 3] gives a value of the longitudinal-mixing coefficient of $2.7 \cdot 10^{-3} \text{ m}^2/\text{sec}$. The results obtained for the flow structure in the liquid phase are in qualitative agreement with the experimental data for crossflow-type bubble plates [2, 11].

The profile of the concentration of *n*-hexane in the liquid phase, calculated by the given model, is presented in Fig. 4 as the isolines in dimensionless form $(C_{\text{liq}} - C_{\text{liq}0}) / (C_{\text{liq}}^* - C_{\text{liq}0})$. As is seen in this figure, the main change in the component concentration occurs at 2/3 of the length of the liquid path on the plate. Near the overflow strip, the efficiency of separation is not high. This fact can be explained by both the decrease in the driving force and the influence of stagnant zones near the column wall. The component-concentration fields in the phases, calculated by the model, are compared to the experimental values at the points of sampling on the plate [20] in Table 1. On the plate under investigation, the liquid flow rate is 913.74 kg/h, while the steam consumption is 277.99 kg/h. In this table, the coordinates of the sampling points are presented in polar [20] and Cartesian coordinates for Fig. 4. Satisfactory agreement between the calculated and experimental data indicates the applicability of the model developed to calculation of the processes of multicomponent rectification on the plate.

Thus, by analyzing the cross motion of the phases, we have constructed a two-dimensional model for the processes of transfer of momentum, mass, and heat in the bubble layer on the plate with overflows. The results of calculation for the velocity fields in the liquid phase performed with the use of the commercial Flow3D package are presented. The results of calculation of the concentration fields are compared to the experimental data for the sieve plate. The model suggested can be used for determining the separative power of the plate in the case of multicomponent rectification in the plate column.

NOTATION

a and a_t , coefficients of molecular and turbulent thermal diffusivity, m^2/sec ; $C_b = 0.6$, constant; C_d , friction factor; C , column vector of the concentrations, mol.fractions; c_p , specific heat, $\text{J}/(\text{kg}\cdot\text{K})$; d_b , bubble diameter, m ; D_t , coefficient of turbulent diffusion, m^2/s ; D , diffusion coefficient, m^2/s ; $\frac{D}{Dt}$, substantive derivative; g , acceleration of gravity, $g = 9.81 \text{ m}/\text{sec}^2$; δG , vapor flow in the volume δV_s , $\delta G = \delta S \rho_g w_g \phi$, kg/s ; H , enthalpy, J/kg ; h_s , height of the static liquid column, m ; $[I]$, unit matrix; K , mass-transfer coefficient, $1/\text{sec}$; K_h , heat-transfer coefficient, $\text{W}/(\text{m}^2\cdot\text{K})$; δM , column vector of the component mass flux in the volume δV_s , $\delta M = r_c \delta V_s$, kg/s ; m , number of components; N , mass flux, $\text{kmol}/(\text{m}^3\cdot\text{sec})$; n , normal to the wall; P , pressure, Pa ; q , heat-flux density, W/m^2 ; q_t , turbulent-heat flux density, W/m^2 ; δQ , heat flux in the volume δV_s , $\delta Q = r_h \delta V_s$, W ; r_c , column vector of the mass sources, $\text{kg}/(\text{m}^3\cdot\text{sec})$; r_p , interaction-force vector, N/m^3 ; r_h , heat source, W/m^3 ; R_1 , Reynolds local number for the viscous sublayer of the diffusion boundary layer; R_e , equivalent aperture radius, m ; S , free area of the column, m^2 ; S_b , area of the apertures (draining area) in the gas-distributing elements, occupied by the gas flow at the entrance to the liquid layer, m^2 ; δS , cross-sectional area of the flow in the volume δV_s , $\delta S = \delta x \delta y$, m^2 ; S_a , active area of the plate, m^2 ; T , temperature, K ; t , time, s ; u_f , dynamic velocity, m/sec ; \mathbf{V} , velocity vector, m/sec ; δV_s , volume of the two-phase mixture, $\delta V_s = \delta S \delta z$, m^3 ; δV_{liq} , volume of the liquid contained in the volume of the two-phase mixture δV_s , $\delta V_{\text{liq}} = \delta V_s (1 - \phi)$, m^3 ; W , mean velocity of the gas in the free area of the column S , m/s ; W_b , mean velocity of the gas in the cross section S_b , m/sec ; u , v and w , longitudinal, transverse, and vertical components of the vector \mathbf{V} , m/sec ; u_τ and u_n , tangential and normal velocity components of the liquid, m/sec ; x , y , and z , longitudinal, transverse, and vertical coordinates on the plate plane; δx , δy , and δz , dimensions of the separated volume of the two-phase flow δV_s on the plate, m ; $y_w = f(x)$, function assigning the shape of the column wall; α_k , volume fraction of the k -phase; α , heat-transfer coefficient, $\text{W}/(\text{m}^3\cdot\text{K})$; β , mass-transfer coefficient, $1/\text{sec}$; μ_{eff} , effective viscosity, $\text{Pa}\cdot\text{s}$; μ and μ_t , coefficients of molecular and turbulent viscosity, $\text{Pa}\cdot\text{sec}$; μ_b , coefficient of turbulent viscosity caused by the bubble motion, $\text{Pa}\cdot\text{sec}$; ν and ν_t , kinematic

and turbulent viscosities, m^2/sec ; ρ , phase density, kg/m^3 ; τ , shear-stress tensor, $\text{kg}/(\text{m}\cdot\text{sec}^2)$; ϕ , gas content; Ξ , correcting factor; Φ , energy dissipation, W/m^3 ; Γ , total mass source, $\text{kg}/(\text{m}^3\cdot\text{sec})$; ε , energy dissipation of the gas flux on the active portion of the jet in the bubble layer, W/m^3 ; ξ , path length of the liquid on the plate, m ; σ , surface tension, N/m ; [...], notation of the matrix; $Sc = \nu/D$, Schmidt number; $Pr = \nu/a$, Prandtl number; $Sc_t = \nu_t/D_t$, turbulent Schmidt number; $Pr_t = a_t/D_t$, turbulent Prandtl number. Superscripts: t, transposition; *, equilibrium; •, nonequimolar; \vee , diagonal matrix. Subscripts: b, bubbling; d, particle; f, friction; e, equivalent; a, active; eff, effective; c, mass transfer; p, pulse; g, gas; k , phase; h, heat transfer; i and j , components; liq, liquid; 0, entrance to the plate; s, interface; t, turbulence; w, wall; τ , tangential component.

REFERENCES

1. V. V. Kafarov, *Principles of Mass Transfer* [in Russian], Moscow (1972).
2. Yu. A. Komissarov, L. S. Gordeev, and D. P. Vent, *Principles of Construction and Design of Industrial Apparatuses: Textbook for Higher School* [in Russian], Moscow (1997).
3. I. A. Aleksandrov, *Mass Transfer in Rectification and Adsorption of Multicomponent Mixtures* [in Russian], Moscow (1975).
4. E. F. Wijn, *Chem. Eng. J.*, **63**, No. 3, 167–180 (1996).
5. N. G. Deen, J. Westerweel, and E. Delnoij, *Chem. Eng. Technol.*, **25**, No. 1, 97–101 (2002).
6. S. Grevsokott and B. H. Sannes, *Chem. Eng. Sci.*, **51**, No. 10, 1703–1713 (1996).
7. M. Ishii, *Thermo-Fluid Dynamic Theory of Two-Phase Flow*, Paris (1975).
8. J. M. Van Baten and R. Krishna, *Chem. Eng. J.*, **77**, No. 3, 143–152 (2000).
9. C. J. Liu, X. G. Yuan, K. T. Yu, and X. J. Zhu, *Chem. Eng. Sci.*, **55**, No. 12, 2287–2294 (2000).
10. G. F. Hewitt, J. M. Delhaye, and N. Zuber (eds.), *Multiphase Science and Technology*, Hemisphere, Washington DC (1987).
11. A. M. Rozen, E. I. Martyushin, and V. M. Olevskii, in: A. M. Rozen (ed.), *Scale Transition in Chemical Technology: Design of Industrial Apparatuses by the Method of Hydrodynamic Modeling* [in Russian], Moscow (1980).
12. S. G. D'yakonov, V. I. Elizarov, and A. G. Laptev, *Theoretical Principles and Modeling of Processes of Separation of Substances* [in Russian], Kazan' (1993).
13. H. L. Toor, *AIChE J.*, **10**, No. 4, 460–465 (1964).
14. W. E. Stewart and R. Prober, *Ind. Eng. Chem. Fund.*, **3**, No. 3, 224–235 (1964).
15. P. Lancaster, *The Theory of Matrices* [Russian translation], Moscow (1982).
16. R. Taylor and R. Krishna, *Multicomponent Mass Transfer*, Wiley, New York (1993).
17. G. Hytoft and R. Gani, *Phase Equilibrium and Separation Processes*, DTH, Lyngby, Denmark (1995).
18. Flow3D, Flow3D. Users Manual Version 7.1 (1997).
19. IMSL, IMSL MATH/LIBRARY User's Manual, Version 3.0, Visual Numerics, Inc., Houston, Texas (1994).
20. G. C. Young and J. Weber, *Ind. Eng. Chem. Process Des. Dev.*, **11**, No. 3, 440–446 (1972).